

# Effect of sequential oxidation on the electronic structure of tungsten clusters

Q. Sun <sup>a</sup>, B.K. Rao <sup>a,\*</sup>, P. Jena <sup>a</sup>, D. Stolcic <sup>b</sup>, G. Ganteför <sup>b</sup>, Y. Kawazoe <sup>c</sup>

<sup>a</sup> *Physics Department, Virginia Commonwealth University, Richmond, VA 23284-2000, USA*

<sup>b</sup> *Department of Physics, University of Konstanz, D-78464 Konstanz, Germany*

<sup>c</sup> *Institute for Materials Research, Tohoku University, Sendai 980-77, Japan*

## Abstract

Using photoelectron spectroscopy and first principles molecular orbital calculations, we report the first observation of an abrupt change in the electronic structure of  $W_4O_m^-$  ( $m \leq 6$ ) clusters at  $m = 5$  which is well below the bulk stoichiometric composition of tungsten oxide ( $WO_3$ ). The signature of this onset is established from an anomalous increase in the vertical detachment energies (VDE), adiabatic electron affinities (AEA), and the energy gaps between highest occupied (HOMO) and lowest unoccupied molecular orbitals (LUMO). These changes are also accompanied by the cleavage of 50% of the W–W bonds and localization of electron charge density in  $W_4O_5$  cluster.

Atomic clusters, which constitute a new phase of matter intermediate between atoms and solids, have attracted considerable interest from researchers over the past three decades. One of the reasons for this continued interest is that clusters can illustrate the evolution of bulk properties one atom at a time. In small clusters the electrons occupy discrete molecular energy levels that are well separated from each other. In addition, a significant gap exists between the highest occupied molecular orbital (HOMO) and lowest unoccupied molecular orbital (LUMO). As clusters grow, these separations, particularly near the HOMO, become increasingly small. Eventually the energy levels of the cluster would resemble the energy bands of the corresponding solid. The most often asked question in this regard is: When is a metal a metal? Arguably, this is a difficult and sometimes ambiguous question since the answer depends on how one defines a metal or a semiconductor atomic cluster. Nevertheless several investigations have been carried out in Hg [1] and Mg [2,3] clusters to address the issue of a change in the electronic structure from insu-

lating to metallic behavior as a function of size. One could argue that when the HOMO–LUMO gaps become small compared to the temperature, the cluster would exhibit metallic behavior. However, as has been seen in Mg clusters [2,3], the HOMO–LUMO gaps open and close with electronic shell closure. Thus, one cannot conclude that a smaller cluster with nearly vanishing HOMO–LUMO gap is metallic while the larger cluster with a non-zero HOMO–LUMO gap is like a semiconductor.

Although it is difficult to clearly label a small atomic cluster as a metal or a semiconductor, there are signatures that distinguish between clusters composed of metal or semiconductor elements. For example, the HOMO–LUMO gaps of clusters of metallic elements tend to be smaller than those of semiconductor elements. Similarly, the electron density distribution of clusters of metallic elements do not show the same degree of directional bonding as is evident in clusters of covalently bonded atoms. In addition, clusters of metallic elements exhibit many low lying isomers (a consequence of flexible bonding characteristics) while the numbers of such isomers of covalently bonded elements are few. Thus based upon these identifying features, one

\*Corresponding author. Fax: +1-804-828-7073.

E-mail address: brao@saturn.vcu.edu (B.K. Rao).

can label the electronic structure of a cluster as ‘metal’-like or ‘semiconductor’-like.

In this Letter, we address this issue by concentrating on tungsten oxide clusters. In particular, we start from a  $W_4$  cluster and study the evolution of its electronic structure as a function of oxygen uptake. We recall that bulk tungsten oxide, which exists in the formula unit  $WO_3$ , is a semi-conductor with a large indirect band gap of 2.62 eV [4]. As oxygen atoms are added to W, at a certain oxygen composition the metal–metal bonds will break and metal–oxygen bonds will form. The resulting bulk metal oxide will then become a semi-conductor or insulator. Note that tungsten oxide remains metallic until a composition of  $WO_{2.72}$ . Similarly if one starts with a tungsten metal cluster and exposes it to an increasing amount of oxygen, eventually all metal–metal bonds will break and an oxide cluster will emerge with a large HOMO–LUMO gap, signifying the transition in their electronic structure. The questions are: at what metal–oxygen composition in clusters does this transition take place? Is this composition the same as that in bulk metal oxide? While significant amount of work has been done on metal–oxide clusters [5–13], no satisfactory answers to the above questions exist.

We have studied this problem by using a combined experimental and theoretical approach. The experiment involves photoelectron spectroscopy of  $W_4O_m^-$  ( $0 \leq m \leq 6$ ) cluster anions while the theory is based on self-consistent field-linear combination of atomic orbitals-molecular orbital (SCF-LCAO-MO) method within the framework of density functional theory (DFT) and generalized gradient approximation (GGA) for exchange-correlation potential. The calculated adiabatic electron affinity (AEA), vertical detachment energies (VDE), and the HOMO–LUMO gaps corresponding to the ground state and low-lying isomers are compared with the experimental data. We find a correlation of AEA, VDE, and HOMO–LUMO gaps with the underlying geometries of the metal oxide clusters as a function of oxygen uptake. In particular, the HOMO–LUMO gaps are small for the bare metal cluster up to an oxygen uptake of  $m = 4$  (a characteristic of ‘metal’-like behavior) and then increase abruptly at  $m = 5$  (a characteristic of ‘semiconductor’-like behavior). This is accompanied by similar variations in the AEAs and VDEs. A study of our optimized geometries shows that at  $W_4O_5$  50% of the metal–metal bonds break and the tetrahedral configuration of  $W_4$  in  $W_4O_m$  ( $m \leq 4$ ) clusters is destroyed. Similarly, an analysis of the HOMO orbitals shows a transition from delocalized behavior in  $W_4O_4$  to localized behavior in  $W_4O_5$ . In addition, while  $W_4O_m$  ( $m \leq 4$ ) clusters possess nearly degenerate isomers, the lowest energy isomers for  $m \geq 5$  lie more than 1.5 eV above the ground states. These results lead us to conclude that a transition in the electronic structure from ‘metal’-like to ‘semiconductor’-like behavior in  $W_4O_m^-$  clusters occurs

at  $m = 5$ , a composition well below the stoichiometric composition of bulk  $WO_3$ . In the following we provide details of our experiment and theory and a discussion of our results.

The experimental set up has been described in detail elsewhere [14,15].  $W_n$  anions are produced with a PACIS (pulsed arc cluster ions source) and mass-selected using a reflectron time-of-flight spectrometer (mass resolution  $m/\Delta m = 400$ ). Molecular oxygen is inserted into the extender to generate  $W_nO_m^-$  clusters. A considerable amount of molecular oxygen is dissociated in the electric arc and, therefore, oxygen atoms are present in the source and for  $W_4O_m^-$  clusters all possible values of  $m$  between  $m = 0$ –12 are observed. The vibrational temperature of the clusters is estimated to be about room temperature. A mass-selected bunch is irradiated by a UV laser pulse ( $h\nu = 4.66$  eV) and the kinetic energies of the detached electrons are measured using a ‘magnetic bottle’-type time-of-flight electron spectrometer. The energy resolution is about 2% corresponding to 20 meV at a kinetic energy of 1 eV. The resulting photoelectron spectra provide information on the electronic structure of the clusters. For example, the peaks in the spectra correspond to vertical transitions from the anion ground state to the allowed states of the neutral having the same geometry as the anion. These transitions occur from the ground state of the anion with spin multiplicity of  $M$ , to the neutral with spin multiplicity of  $M' = M \pm 1$ . The peaks in the spectra can be broad following transition from the anion to the electronic and vibrational excited states of the neutral if the ground state geometries of anion and neutral are very different.

The photoelectron spectra also provide an estimate of the size of the HOMO–LUMO gaps of the neutral clusters in the geometry of the anion. The peak at lowest binding energy corresponds to the transition to the ground state of the neutral cluster, while the peak next higher in energy corresponds to the transition to the first excited state of the neutral both at the anion geometry. The distance between the two features is assigned to the energy of the first excited state of the neutral, which corresponds in the language of solid state physics to the semiconductor band gap. In molecules, this excitation energy strongly correlates with the HOMO–LUMO gap [16]. These two quantities are equal in the frozen orbital picture. The HOMO–LUMO gap is usually defined as the energy difference between the HOMO and the LUMO in the neutral ground state. The binding energies of both orbitals change due to relaxation and correlation effects, if one electron is excited from the HOMO into the LUMO, which is the first excited state of the particle. In the frozen orbital picture, these effects are neglected.

In Fig. 1a we plot the photoelectron spectra of  $W_4O_m^-$  ( $0 \leq m \leq 6$ ) clusters. The spectra of  $W_4$  are characterized by a somewhat broadened single peak lying at 1.79 eV.

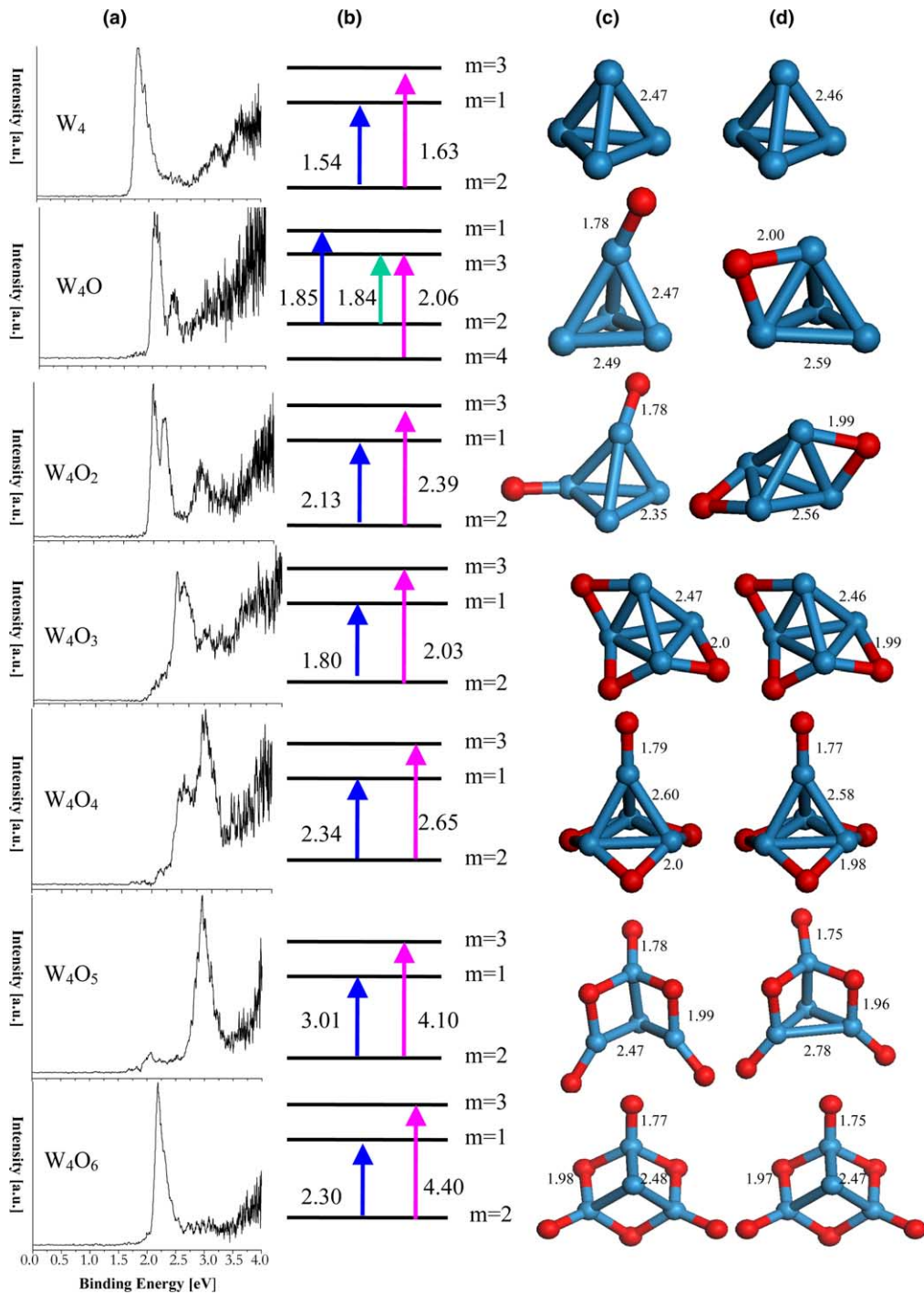


Fig. 1. (a) Experimental photodetachment spectra. (b) The calculated transitions from the ground state of the anion with spin multiplicity  $M$  to neutrals at the anion geometry with multiplicities of  $M \pm 1$ . Note that the energy levels are not drawn to scale. (c) Geometries of the ground state for anion and (d) for neutral clusters. The only exceptions are  $W_4$  and  $W_4O_3^-$  where the nearly degenerate isomers are shown. Some sample bond lengths in Å are given in (c) and (d).

The spectra of  $W_4O^-$  to  $W_4O_4^-$ , on the other hand, exhibit a double peak structure. A significant change in the spectra is noticed for  $W_4O_5^-$  and  $W_4O_6^-$ . In the spectra of  $W_4O_3$ ,  $W_4O_4$  and  $W_4O_5$  weak features at low binding energies are observed (e.g., at 2.0 eV for  $W_4O_5$ ). We assign these features to different, less abundant isomers,

which here will be neglected for simplification and discussed in detail elsewhere. The main peak of the  $W_4O_5^-$  spectra shifts to higher energy while that of  $W_4O_6^-$  becomes narrow. For a quantitative analysis of these spectra we list the measured vertical detachment energies (corresponding to the low energy peak) in

Table 1

Calculated and experimental vertical detachment energy (VDE), adiabatic electron affinity (EA), and HOMO–LUMO gap (in eV) as a function of oxygen uptake

Quantity		Oxygen content					
		$m = 1$	$m = 2$	$m = 3$	$m = 4$	$m = 5$	$m = 6$
VDE	Theo.	2.10	2.13	2.03	2.34	3.01	2.30
	Expt.	2.07	1.98	2.32	2.46	2.96	2.19
EA	Theo.	1.78	1.82	1.88	2.01	2.73	2.18
	Expt.	1.92	1.89	2.18	2.27	2.70	2.08
Energy gap	Theo.	0.22	0.26	0.23	0.31	1.10	2.10
	Expt.	0.32	0.23	0.13	0.28	1.16	1.90

Table 1. The adiabatic electron affinities that measure the energy difference between the ground states of the anion and neutral are also given in Table 1. We note that the electron affinity and vertical detachment energies increase significantly from  $W_4$  to  $W_4O$ . As subsequent oxygen atoms are added, there is a monotonic increase in VDE and AEA which is characteristic of metal-like behavior [5–8,12,13]. However at  $W_4O_5$ , there is an abrupt increase in both VDE and AEA. This trend is also seen in the HOMO–LUMO gaps in Table 1.

To understand the correlation between these energies and the underlying bonding characteristics, accurate information on the equilibrium geometries of these clusters is needed. No experimental technique exists at this time to provide such information. The only route to obtain information on geometry is through theoretical calculation. We describe that procedure in the following and validate the accuracy of our calculation by comparing calculated electron affinities, vertical detachment energies, and HOMO–LUMO gaps with the experimental data.

We have used the self-consistent field-linear combination of atomic orbital-molecular orbital (SCF-LCAO-MO) approach. The total energies are calculated using DFT and Becke, Perdew, Wang prescription (commonly referred to as BPW91) for the generalized gradient approximation (GGA) for exchange–correlation potential. The atomic orbitals are represented by a Gaussian basis. We have used the 6-311G\* basis set for oxygen and the Stuttgart relativistic effective core potential basis set for tungsten [17]. The structures for the anion and neutral clusters were optimized without symmetry constraint using the GAUSSIAN 98 code [18]. Several starting configurations were used in the geometry optimization of each cluster. These included oxygen bonded to the on-top site, bridge site, interior site, as well as inserted into metal–metal bonds. As oxygen concentration increases, we allowed the possibility that different oxygen atoms can bind to different sites as well. The converged energies not only allow us to determine the ground state of the anion and neutral clusters, but also to identify their low-lying isomers. The details of these results will

be published elsewhere. In the following we only discuss the salient features of our results.

We first discuss the geometries of the anionic and neutral  $W_4O_m$  ( $0 \leq m \leq 6$ ) clusters. These are given in Fig. 1c,d, respectively. The ground state of  $W_4^-$  has two energetically degenerate structures: a perfect tetrahedron with  $T_d$  symmetry and a Jahn–Teller distorted structure (bent rhombus) with  $D_{2d}$  symmetry. The ground state of neutral  $W_4$  also exhibits two nearly degenerate structures. The isomer displayed in Fig. 1d has tetrahedral structure and lies 0.12 eV above the  $D_{2d}$  ground state structure. It should be noted that the quantitative accuracy of our calculated results is limited by the choice of exchange–correlation energy functional, the lack of a full relativistic treatment of tungsten, and the basis sets. From a systematic comparison of our theory with experiment which will follow, we set the limit of the accuracy of our calculated results at 0.2 eV. Thus any isomer that lies within this energy range from the ground state can be regarded as nearly degenerate and could very well be observed experimentally.

$W_4O^-$  cluster possesses two nearly degenerate structures: in both these structures the oxygen is bonded to a single metal atom at the on-top site but their spin multiplicities are different. The ground state is quartet while the doublet state lies only 0.2 eV above it. The neutral  $W_4O$  also exhibits two nearly degenerate structures, but here the oxygen bonded to the on-top site lies 0.10 eV above the bridge bonded ground state structure. The anionic and neutral  $W_4O_2$  clusters exhibit unique ground state geometries with the next higher energy isomers lying respectively 0.54 and 0.38 eV above ground state structures.  $W_4O_3^-$  has two nearly degenerate structures. The isomer with all bridge bonded oxygen is 0.14 eV above the ground state structure where all the oxygen atoms are bonded to the on-top site. In Fig. 1c we give the bridge bonded isomer instead of the ground state structure. As we will discuss later the transition energies of this isomer are consistent with experiment, and according to our calculational accuracy, it is energetically degenerate. The neutral  $W_4O_3$  has a clearly defined ground state where all the oxygen

atoms are bridge bonded. The ground state of  $W_4O_4^-$  contains three bridge-bonded and one on-top oxygen where the isomer with all the bridge-bonded oxygen atoms lies 0.21 eV above the ground state. It is important to note that in all these clusters, the  $W_4$  unit remains intact upon oxidation. The geometries of  $W_4O_5$  and  $W_4O_6$  undergo a sudden transformation: the tetrahedral  $W_4$  unit breaks leading to a ring-like structure with a fewer metal–metal bonds. The neutral and anion have the same structures and oxygen binds to on-top and bridge positions in equal proportion in  $W_4O_6$ . The geometry of  $W_4O_6$  is the most symmetric of all the metal–oxygen clusters studied. The isomers of these clusters lie more than 1.5 eV above the corresponding ground states.

We have computed the vertical detachment energies by calculating the total energies of neutral clusters having the same geometries as their counter anions in Fig. 1c, but with spin multiplicities differing from the anion by  $\pm 1$ . With exception of  $W_4O^-$ , all the anions studied here have spin multiplicities of 2. As noted earlier  $W_4O^-$  has a nearly degenerate isomer with spin multiplicity of 4. Calculated vertical transitions from doublet anion to singlet and triplet neutrals are plotted in Fig. 1b. For  $W_4O^-$  we also list the transitions from quartet anion to triplet neutral. The transition from quartet  $W_4O^-$  to quintet  $W_4O$  lies at 2.94 eV. The calculated vertical detachment energies corresponding to the lower transition energies and adiabatic electron affinities are compared with experiment in Table 1. Note that the agreement is very good. The trend is reproduced well and quantitatively the calculated results are within 0.2 eV of the experiment. Most importantly, a sharp increase in the VDEs and AEAs at  $W_4O_5$  agree very well with experiment. And this feature coincides with the structural transformation of the  $W_4$  unit from tetrahedral to ring-like motif.

The energy difference between the two transitions given in Fig. 1b are listed in Table 1. This has been identified in the experiment as the HOMO–LUMO gap. We note that these energies are around 0.2 ~ 0.3 V for  $W_4O^-$  to  $W_4O_4^-$ , but abruptly increases to 1.1 eV in  $W_4O_5^-$ . This is a clear indication that there is a fundamental change in the electronic structure in going from  $W_4O_4^-$  to  $W_4O_5^-$ . To further corroborate this finding, we have calculated the HOMO orbitals in  $W_4O_4$  and  $W_4O_5$ . The HOMO in  $W_4O_4$  is mainly contributed by W atoms and the electron distribution is delocalized as is expected for metallic bonding. In  $W_4O_5$ , on the other hand, the cleavage of some of the W–W bonds makes the electrons much more localized. The HOMO is composed primarily of contributions from the oxygen atoms and three of the tungsten atoms still bonded. The details of the charge distributions will be published later.

According to our results for  $W_4O_m$  the transition from metal-like to oxide-like behavior starts at  $m = 5$

and  $W_4O_6$  has a HOMO–LUMO gap of 2.23 eV. This is comparable to the indirect band gap of the bulk material (2.62 eV). Compared to bulk  $WO_3$  oxide,  $W_4O_6$  corresponds to 50% deficiency of oxygen (=  $WO_{1.5}$ ). Studies on nonstoichiometric bulk tungsten oxides reveal that  $WO_{2.72}$  with a relatively small oxygen deficiency is metallic [19,20].

Bulk  $WO_3$  consists of octahedral  $WO_6$  building blocks. Each W atom is surrounded by six oxygen atoms forming an octahedron and neighboring octahedra share the corner oxygen atoms. For  $WO_3$  clusters on surfaces, three-membered rings of such octahedra are observed [21]. The three W atoms are connected via oxygen atoms forming a regular triangle with W–O–W sides and each W atom has two O atoms bound on-top in plane. Most likely, this is the structure of  $W_3O_9$  too, which is the most abundant product from Knudsen cell effusion of bulk  $WO_3$  [22].  $W_4O_5$  and  $W_4O_6$  have a similar triangular structure with the W atoms connected by O bridges (Fig. 1). This triangular motif seems to be a preferred structure of  $WO_3$ . As in the case of  $C_{60}$ , a peculiar geometry combined with a high symmetry result in a large HOMO–LUMO gap and a high stability of  $W_4O_6$ .

In summary we show, through a combined experimental and theoretical study, that the electronic structure of  $W_4O_m$  clusters undergo a transition from ‘metal’-like to ‘semiconductor’-like behavior with oxygen uptake at  $m = 5$ . This composition (125% of oxygen) occurs well below the bulk composition of tungsten oxide, namely 300% of oxygen. This shows that atomic clusters with most of their atoms on the surface react differently with oxygen than their bulk does. Since bulk metal–oxide play an important role in catalysis, it is possible that metal–oxide clusters may have unique catalytic properties, but at much smaller oxygen composition. In addition, we have shown that a systematic study of the vertical detachment energies, adiabatic electron affinities, and HOMO–LUMO gaps could be used as characteristic signatures to identify changes in the nature of bonding.

## Acknowledgements

Work at Virginia Commonwealth University was supported in part by a grant (DEFG02-96ER45579) from the Department of Energy.

## References

- [1] R. Busani, M. Folkers, O. Cheshnovsky, Phys. Rev. Lett. 81 (1998) 3836.
- [2] O.C. Thomas, W.J. Zheng, S.J. Xu, K.H. Bowen, Phys. Rev. Lett. 89 (2002) 213403.
- [3] P. Acioli, J. Jellinek, Phys. Rev. Lett. 89 (2002) 213402.

- [4] F.P. Koffyberg, K. Dwight, A. Wold, *Solid State Commun.* 30 (1979) 433.
- [5] L.-S. Wang, H. Wu, S.R. Desai, *Phys. Rev. Lett.* 76 (1996) 4853.
- [6] M. Gutowski, P. Skurski, Xi Li, L.-S. Wang, *Phys. Rev. Lett.* 85 (2000) 3145.
- [7] S.R. Desai, H. Wu, C.M. Rohlfing, L.-S. Wang, *J. Chem. Phys.* 106 (1997) 1309.
- [8] H. Wu, X. Li, X.B. Wang, C.F. Ding, L.-S. Wang, *J. Chem. Phys.* 109 (1998) 449.
- [9] S.K. Nayak, P. Jena, *Phys. Rev. Lett.* 81 (1998) 2970.
- [10] P.J. Ziemann, A.W. Castlemann Jr., *J. Chem. Phys.* 94 (1991) 718.
- [11] G.L. Gutsev, P. Jena, H.J. Zhai, L.-S. Wang, *J. Chem. Phys.* 115 (2001) 7935.
- [12] Q. Sun, M. Sakurai, Q. Wang, J.Z. Yu, H. Wang, K. Sumiyama, Y. Kawazoe, *Phys. Rev. B* 62 (2000) 8500.
- [13] Q. Wang, Q. Sun, M. Sakurai, J.Z. Yu, B.L. Gu, K. Sumiyama, Y. Kawazoe, *Phys. Rev. B* 59 (1999) 12672.
- [14] H. Handschuh, G. Ganteför, W. Eberhardt, *Rev. Sci. Instrum.* 66 (1995) 3838.
- [15] S. Burkart, N. Blessing, B. Klipp, J. Müller, G. Ganteför, G. Seifert, *Chem. Phys. Lett.* 301 (1999) 546.
- [16] See for reference H. Kietzmann, R. Rochow, G. Ganteför, W. Eberhardt, K. Vietze, G. Seifert, P.W. Fowler, *Phys. Rev. Lett.* 81 (1998) 5378.
- [17] M. Dolg, H. Stoll, H. Preuss, R.M. Pitzer, *J. Phys. Chem.* 97 (1993) 5852.
- [18] M.J. Frisch et al., *GAUSSIAN 98: Gaussian*, Pittsburgh, PA, 1998.
- [19] B.A. de Angelis, M. Schiavello, *J. Solid State Chem.* 21 (1977) 67.
- [20] H. Höchst, R.D. Bringans, *Appl. Surf. Sci.* 11/12 (1982) 768.
- [21] G.G. Granquist, *Appl. Phys. A* 57 (1993) 3.
- [22] J. Berkowitz, W.A. Chupka, M.G. Inghram, *J. Chem. Phys.* 27 (1957) 85.